Role of Au^+ in Supporting and Activating Au_7 on $TiO_2(110)$

J. G. Wang and B. Hammer

Interdisciplinary Nanoscience Center (iNANO) and Department of Physics and Astronomy, University of Aarhus, DK 8000 Aarhus C, Denmark

(Received 14 June 2006; published 29 September 2006)

The adhesion properties and catalytic activity of rutile $TiO_2(110)$-supported Au_7 nanoclusters in different oxidation states are investigated by means of density functional theory. The calculations cover both surface science conditions of reduced TiO_2 and real catalyst conditions of oxidized (alkaline) TiO_2 supports. Large adhesion energies of Au_7 are found only when modeling real catalysts where the cluster becomes cationic with Au^+ ions in Au-O or Au-OH bonds. The full catalytic cycle for oxidation of CO by O_2 over Au_7 on alkaline $TiO_2(110)$ is calculated and found to involve only small activation barriers. In the presence of the CO reductant, the Au^+ sites are capable of cycling between bonding of atomic and molecular oxygen. We confirm our findings by comparison of calculated and experimental infrared stretch frequency data for adsorbed CO.

DOI: 10.1103/PhysRevLett.97.136107 PACS numbers: 68.47.Jn, 68.43.Fg, 82.65.+r

Oxide-supported gold nanoparticles have been shown to catalyze a range of reactions, including CO oxidation [1], propylene epoxidation [2], and the water gas shift reaction [3]. The chemistry of the gold nanoparticles is thus in stark contrast to that of bulk gold surfaces, since these are considered catalytically inactive [4]. Using the surface science approach, a number of mechanisms have been proposed explaining the high activity of the gold nanoparticles. These include quantum size effects of two-layer Au islands [5], negative charging of the Au clusters [6,7], abundance of low Au-Au coordination sites [8], and the presence of Au-support periphery sites [9–11]. In all these works, an anionic nature of the Au particles was inferred. In the present work, we adapt a more realistic view of what the real gold-support interface looks like after preparation and under reaction conditions. We propose that Au nanoparticles are slightly oxidized having cationic Au^+ sites. We identify Au^+-O adhesion bonds of a mixed covalent and ionic nature. Similar Au^+-O_2 bonds at the Au-support periphery sites [9–11] are suggested to be responsible for the catalytic activity of Au nanoparticles in oxidation reactions.

Two very efficient preparation techniques for supported Au nanoparticle catalysts are coprecipitation and deposition-precipitation. In the former, both support and gold precursors are extracted from solution; in the latter, a preformed support is employed for the precipitation of the gold precursor. The precipitation is most efficient for a *p*H value of 9 [12], and it is believed that the gold precursors are hydroxyls [13]. Pretreatment in the form of calcination (heating in air) at moderate temperatures is often employed to transform the gold precursors into catalytically active metallic gold attached to crystalline metal oxide supports [14,15]. The precise state of the gold particles after the calcination and under reaction conditions is subject to debate. Contrary to most surface science studies, Bond and Thompson [16] and others [17,18] have suggested that the Au particles are oxidized with Au^+ or Au^{3+} sites at the particle-support interface being responsible for the catalytic activity.

Comparing the activity of Au nanoparticles on different supports, a clear trend is found: Very acidic materials (for example, Al_2O_3-SiO_2 and WO_3) show poor activity, less acidic (SiO_2, Al_2O_3, and TiO_2) or slightly basic materials (Fe_2O_3, Co_3O_4, and NiO) show high activity, while strongly alkaline materials [$Be(OH)_2$ and $Mg(OH)_2$] exhibit the highest activity [13]. Considering that the more basic the support, the more oxidized the supported Au particles are expected to be, this trend calls for further consideration of cationic Au particles.

To model gold nanoparticles under different oxidation conditions, we have performed density functional theory (DFT) calculations [19] of gold clusters on supports in various oxidation states. As the support, we choose rutile $TiO_2(110)$, which has proven very efficient [13,20]. For the Au nanoparticles, we select Au_7, which is the smallest Au cluster on rutile $TiO_2(110)$ with a measurable reaction rate for CO combustion [21]. The structure of the $TiO_2(110)$ surface is illustrated in Fig. 1(a). The $TiO_2(110)$ has protruding oxygen atoms (O_{br}) that bridge Ti atoms underneath (not shown). These Ti atoms coordinate to six oxygen atoms as any other Ti in bulk TiO_2. The surface further has coordinatively unsaturated Ti atoms (Ti_{5c}) that coordinate only to five oxygen atoms.

In the calculations, the different oxidation states considered for the $TiO_2(110)$ range all the way from highly reduced to highly oxidized. The reduced surfaces contain either bridging oxygen vacancies (O_{vac}) or bridging hydroxyl groups (OH_{br}). To avoid confusion with other hydroxyl groups, we refer to these species as capping H atoms (H_{cap}). The oxidized states of the surface are modeled by alkaline $TiO_2(110)$ having terminal OH groups (OH_{tr}) atop the Ti_{5c} in the troughs. The OH_{tr} are allowed to dissociate forming terminal O (O_{tr}) on the Ti_{5c} sites and capping H on the O_{br} sites (i.e., OH_{br} groups). We envisage the hydroxyls as originating from the Au precursors. The

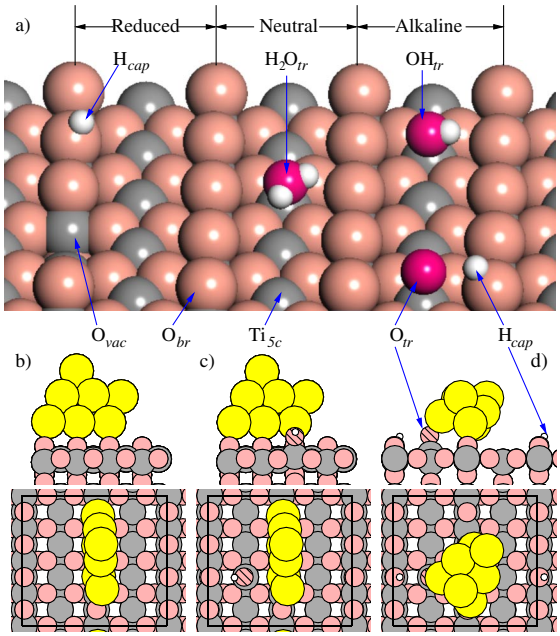

FIG. 1 (color online). (a) Schematic of the rutile $TiO_2(110)$ surface. Most stable structures of Au_7 on (b) stoichiometric TiO_2 and alkaline TiO_2 with (c) intact or (d) dissociated OH_{tr}.

calcination pretreatment clearly removes hydroxyls from the catalyst, but only to the point that is thermodynamically preferred at the elevated temperature [22]. The possible influence of a humid environment is investigated by inclusion in some cases of an adsorbed water molecule (H_2O_{tr}) on the Ti_{5c} sites.

The adhesion potential energies for the calculated most stable 2D or 3D Au_7 clusters supported on $TiO_2(110)$ are given in Table I, and some of the structures are shown in Figs. 1(b)–1(d). More structures are shown in Ref. [23], Figs. S1–S6. On $TiO_2(110)$ in most oxidation states, we find the Au_7 to prefer a 2D structure as in the gas phase [24]. The binding of the 2D clusters is, however, weak on the reduced TiO_2 that has a vacancy or an H_{cap}. On stoichiometric $TiO_2(110)$, the 2D cluster [Fig. 1(b)] shows increased stability ($E_{adh} = -1.18$ eV) and a 3D structure becomes slightly stable (-0.17 eV) against desorption as a 2D cluster. The weak binding is consistent with previous findings with DFT of small adhesion energies of extended gold structures on stoichiometric $TiO_2(110)$ [11,25].

TABLE I. Adhesion potential energy E_{adh} of the most stable 2D and 3D Au_7 cluster on different $TiO_2(110)$ surfaces.

$TiO_2(110)$	Au_7 (2D)	Au_7 (3D)
Vacancy	−0.52	0.27
H_{cap}	−0.87	0.10
Stoichiometric	−1.18	−0.17
OH_{tr}	−2.34	−2.07
$OH_{tr} + H_2O_{tr}$	−2.38	−2.11
$O_{tr} + H_{cap}$	−2.28	−2.42
$O_{tr} + H_{cap} + H_2O_{tr}$	−2.38	−2.40

The alkaline $TiO_2(110)$ surfaces show markedly larger stability of the Au clusters. In this case, the 2D cluster is bonded by about 2.3 eV [Fig. 1(c)], and, depending on whether OH_{tr} or $O_{tr} + H_{cap}$ species are present, the binding of 3D clusters [Fig. 1(d)] amounts to 2.1 and 2.4 eV. For these situations, we also included a water molecule in some of the calculations. However, no great effect of an H_2O_{tr} coadsorbate is identified (cf. Table I).

The bonding mechanism and charge state of two of the supported Au_7 clusters is analyzed in Fig. 2. First, the charge density change induced upon adsorption of 2D (or 3D) Au_7 and OH_{tr} (or $O_{tr} + H_{cap}$),

$$\Delta\rho(\mathbf{r}) = \rho_{\mathrm{Au/TiO2\text{-}OH_{tr}}}(\mathbf{r}) - \rho_{\mathrm{Au}}(\mathbf{r}) - \rho_{\mathrm{TiO2}}(\mathbf{r}) - \rho_{\mathrm{OH}}(\mathbf{r}),$$

is shown in Figs. 2(a) and 2(b), from which the positive charging state (blue isosurfaces) of particularly 1st layer Au atoms in the Au_7 on alkaline $TiO_2(110)$ is obvious. Next, the projected density of states (pDOS) on some of the Au($5d$)-O_{tr}($2p$) and Au($5d$)-O_{br}($2p$) σ bonds of the 3D Au_7 cluster on $TiO_2(110)$ with $O_{tr} + H_{cap}$ [Figs. 1(d) and 2(b)] are shown in Fig. 2(c). These plots are suggestive of a mixed covalent and ionic Au-O interaction, which is confirmed by the plotting of some individual Kohn-Sham orbitals, ψ_1, ψ_2, and ψ_3, in Fig. 2(d). Orbitals ψ_1 and ψ_3 are clearly identifiable as σ bonds between the Au and the O_{tr} and O_{br} atoms, respectively, while orbital ψ_2 is of an antibonding nature, mainly with the weight on the Au sites. Since ψ_2 has an energy above the Fermi level [cf. Fig. 2(c)], it is depleted, whereby the Au becomes cationic as seen in the charge density difference plot [Fig. 2(b)]. The excess electron charge ends up in O_{tr} and O_{br} dangling bonds [Fig. 2(b)] or in Au-O bonding states of mainly oxygen character (e.g., ψ_1 or ψ_3), whereby the O atoms become negatively charged. The present analysis allows for a quantitative explanation for the stronger adhesion of Au_7 on the alkaline surface; the total Au($5d$) population is lowered by $0.49e^-$ on alkaline TiO_2 but only by 0.23–$0.26e^-$ on stoichiometric or reduced TiO_2, meaning that, on the alkaline TiO_2, the antibonding Au-O bonds are less filled and, hence, the adhesion enhanced.

We note that cationic Au^+ species have been detected by a range of experimental techniques for Au clusters supported on various supports (Fe_2O_3, TiO_2, and Al_2O_3) [15,16,26].

We now turn to investigate if the strongly bound Au_7 cluster on the *alkaline* TiO_2 is catalytically active. In Fig. 3, the calculated catalytic cycle of $2CO + O_2 \rightarrow 2CO_2$ is shown for the 3D Au_7 cluster on the $TiO_2(110)$-O_{tr}-H_{cap} surface. Since every reaction step is exothermic by at least 0.5 eV and only minute energy barriers (0.16 and 0.01 eV) are calculated for the CO_2 formation reactions, the calculations do predict that the cationic Au_7 can be highly active on an alkaline $TiO_2(110)$ support.

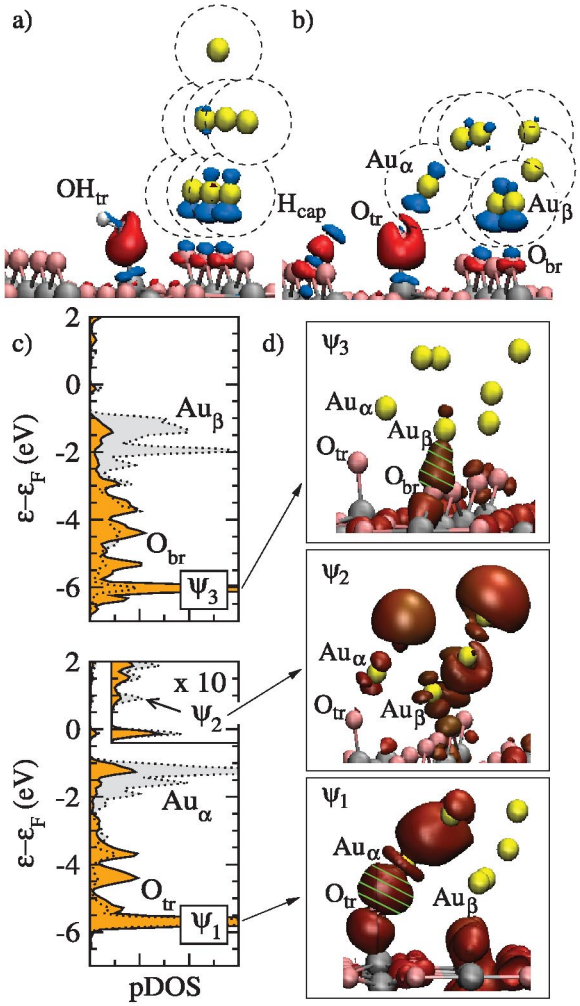

FIG. 2 (color). (a),(b) Induced charge rearrangements upon adsorption of Au_7 and OH_{tr} (or $O_{tr} + H_{cap}$) for the configurations shown in Figs. 1(c) and 1(d). Blue (red) isosurfaces indicate depletion (addition) of $0.05e^-/Å^3$. Yellow spheres and dashed circles mark the Au positions. (c) Electronic DOS projected onto Au($5d_{z^2}$) (gray) and O($2p_z$) (orange) orbitals with the z axis parallel to the Au_α-O_{tr} and Au_β-O_{br} bonds, respectively. (d) Isosurfaces of the amplitude of selected Kohn-Sham orbitals, ψ_{1-3}. Covalent bonds are hatched in green.

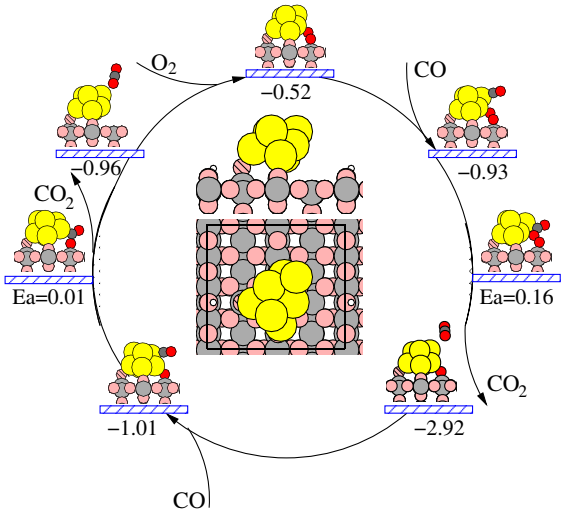

FIG. 3 (color online). Catalytic cycle for CO oxidation at Au_7 supported on alkaline TiO_2(110) with $O_{tr} + H_{cap}$.

The adsorption configurations and transition states along the reaction path are included in Fig. 3. The O_2 is seen to bind at the Au-TiO_2 interface in agreement with previous reports on reduced supports [7,9–11] and the CO binds to 2nd layer Au^0 sites. The O_2 further depletes the $Au_7(5d)$ states by $0.22e^-$ (to a total value of $0.71e^-$) suggesting a bonding mechanism similar to that for O_{tr} discussed in Fig. 2. After the first CO_2 formation, one oxygen atom from the O_2 is left on the catalyst particle and forms a Au-O bond much similar to the one formed by the original O_{tr}. The presence of the second O_{tr} is causing a depletion of the $Au_7(5d)$ states by $0.33e^-$ (i.e., totally by $0.82e^-$) exceeding the depletion from 0.26 to $0.49e^-$ originating from the first O_{tr}. When the Au_7 is bonded in this way by *two* O_{tr}, either of them may easily be removed by the 2nd CO, thereby forming CO_2 and closing the cycle. We note that, in experiments with an isotope labeled O_2, it might therefore well appear that an "apparent" lattice O (our O_{tr}) is involved in the reaction [14]. We also note that a 3rd CO is unlikely to fully reduce the Au_7 by removing the last O_{tr}. According to Table I, the 3D Au_7 is 2.5 eV less stable without this stabilizing O_{tr}, but adsorption of CO and formation of CO_2 in a 2nd step releases only $1.01 + 0.96 \simeq 2.0$ eV. As an important finding in Fig. 3, the Au^+ ions at the gold-oxide interface show a remarkable ability to bind both O_2 and atomic O, so that all steps in the CO oxidation become exothermic. More reactive metals than gold would most likely bind the atomic O too strongly, meaning that a catalytic cycle in which the O_2 and O are sequentially sharing the same site would become inhibited.

The catalytic cycle of Fig. 3 shows that indeed the Au_7 cluster under alkaline conditions is expected to be highly active. We cannot make a similar statement for Au_7 on reduced or stoichiometric surfaces, since the 2D Au_7 structure prohibits efficient O_2 adsorption. In fact, on the stoichiometric support, we do not identify a stable binding site for the O_2 on the 2D Au_7 cluster [Fig. 1(b)]. If a 3D Au_7 structure is enforced on the stoichiometric TiO_2(110), we do, however, find the O_2 to bind with 0.40 eV, which is comparable to the 0.52 eV O_2 binding on 3D Au_7 at alkaline TiO_2(110). In calculations where H_2O_{tr} is included to model the role of a wet environment, we further identify improved O_2 binding (0.61 eV) and favorable energetics for the entire catalytic cycle (see Ref. [23], Fig. S7). This agrees well with reports on a promoting effect of water on the CO oxidation reaction [27].

Finally, we have calculated the CO stretch frequencies for a number of CO adsorption configurations (Fig. 4). The calculated frequencies fall in two groups: CO's that bind to Au^0 sites [Figs. 4(a)–4(c)] have frequencies in the range

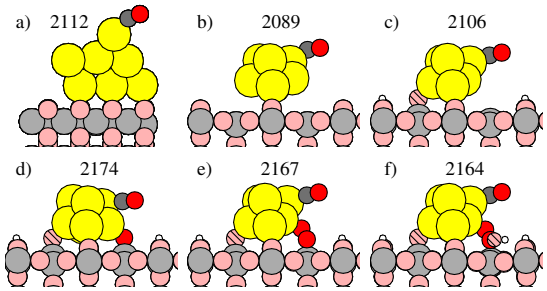

FIG. 4 (color online). Calculated vibrational stretch frequencies (in cm^{-1}) for CO adsorbed on (a),(b) 2D and 3D Au_7 clusters on stoichiometric TiO_2, (c) Au_7 having one Au-O_{tr} bond, (d) Au_7 having two Au-O_{tr} bonds, and (e),(f) Au_7 having one Au-O_{tr} and one Au-O_2 bond without or with coadsorbed H_2O_{tr}.

2089–2112 cm^{-1}, while CO's that bind to Au atoms that are *neighboring* Au^+ atoms in Au-O or Au-O_2 bonds [Figs. 4(d)–4(f)] have frequencies in the range 2164–2174 cm^{-1}. These results fully corroborate the infrared frequencies found in a number of experimental studies [14,28–30]. In these works, typical stretch frequencies of CO on a supported gold catalyst were found in the range of 2101–2110 and 2168–2176 cm^{-1} and were attributed CO bound to Au^0 and Au^+ sites, respectively.

In the present work, some effort was spent comparing supported 2D and 3D clusters. We note, however, that for larger clusters, the 2D to 3D transition is not an issue since the clusters already prefer the 3D shape in the gas phase [24].

In summary, we have used density functional theory calculations to identify that strong Au-oxide support adhesion is obtained on oxidized (alkaline) $TiO_2(110)$ surfaces but not on reduced or stoichiometric $TiO_2(110)$. The Au clusters become cationic as a result of the formation of the Au-O adhesion bonds. The investigated cationic Au_7 cluster is capable of binding both molecular and atomic oxygen at perimeter sites next to the support and CO further away from the support, and the adsorbates are found to react with small energy barriers.

We acknowledge discussions with S. Wendt, D. Matthey, and F. Besenbacher and support from the Danish Research Councils and Dansk Center for Scientific Computing.

[1] M. Haruta, N. Yamada, T. Kobayashi, and S. Iijima, J. Catal. **115**, 301 (1989).
[2] T. Hayashi, K. Tanaka, and M. Haruta, J. Catal. **178**, 566 (1998).
[3] F. Boccuzzi, A. Chiorino, M. Manzoli, D. Andreeva, and T. Tabakova, J. Catal. **188**, 176 (1999).
[4] B. Hammer and J. K. Nørskov, Nature (London) **376**, 238 (1995).
[5] M. Valden, X. Lai, and D. W. Goodman, Science **281**, 1647 (1998).
[6] B. Yoon *et al.*, Science **307**, 403 (2005).
[7] I. N. Remediakis, N. Lopez, and J. K. Nørskov, Angew. Chem., Int. Ed. **44**, 1824 (2005).
[8] M. Mavrikakis *et al.*, Catal. Lett. **64**, 101 (2000).
[9] L. M. Molina *et al.*, Phys. Rev. Lett. **90**, 206102 (2003).
[10] Z. P. Liu *et al.*, Phys. Rev. Lett. **91**, 266102 (2003).
[11] L. M. Molina *et al.*, J. Chem. Phys. **120**, 7673 (2004).
[12] F. Moreau, G. C. Bond, and A. O. Taylor, J. Catal. **231**, 105 (2005).
[13] M. Haruta, J. New Mater. Electrochem. Syst. **7**, 163 (2004).
[14] F. Boccuzzi, A. Chiorino, M. Manzoli, P. Lu, T. Akita, S. Ichikawa, and M. Haruta, J. Catal. **202**, 256 (2001).
[15] N. A. Hodge *et al.*, Catal Today **72**, 133 (2002).
[16] G. C. Bond and D. T. Thompson, Gold Bulletin (London) **33**, 41 (2000).
[17] C. K. Costello, M. C. Kung, H. S. Oh, Y. Wang, and H. H. Kung, Appl. Catal., A **232**, 159 (2002).
[18] J. Guzman and B. C. Gates, J. Phys. Chem. B **106**, 7659 (2002).
[19] The DACAPO package (http://www.camp.dtu.dk/campos) with a plane-wave basis set (Ecut = 25 Ry) and ultrasoft pseudopotentials was used. The revised Perdew-Burke-Ernzerhof functional [31] was employed for exchange-correlation effects. A (4×2) $TiO_2(110)$ surface unit cell comprising slabs of three trilayers (the first of which being fully relaxed) at the theoretically derived lattice constants ($a = 4.69$ Å, $c = 2.99$ Å, and $u = 0.305$) was adopted. The Au_7 adhesion potential energy is calculated as: $E_{adh} = E(Au_7 + TiO_2) - E(Au_7) - E(TiO_2)$, where $E(Au_7 + TiO_2)$, $E(Au_7)$, and $E(TiO_2)$ are the total energies of the combined systems, the most stable gas phase Au_7 2D cluster, and the TiO_2 surface in a given oxidation state, respectively. Transition states are located by constrained relaxation. The calculated vibrational frequencies have been scaled by 0.9821, which is the ratio between the measured (2143 cm^{-1}) and calculated (2182 cm^{-1}) stretch frequencies for gas phase CO.
[20] T. V. W. Janssens, A. Carlsson, A. Puig-Molina, and B. S. Clausen, J. Catal. **240**, 108 (2006).
[21] S. Lee, C. Fan, T. Wu, and S. L. Anderson, J. Am. Chem. Soc. **126**, 5682 (2004).
[22] A. S. Barnard, P. Zapol, and L. A. Curtiss, Surf. Sci. **582**, 173 (2005).
[23] See EPAPS Document No. E-PRLTAO-97-037640 for additional illustrations of configurations considered [adds to the configurations in Figs. 1(b)–1(d) in the Letter]. For more information on EPAPS, see http://www.aip.org/pubservs/epaps.html.
[24] L. Xiao and L. C. Wang, Chem. Phys. Lett. **392**, 452 (2004).
[25] N. Lopez and J. K. Norskov, Surf. Sci. **515**, 175 (2002).
[26] L. Fu *et al.*, J. Phys. Chem. B **109**, 3704 (2005).
[27] M. M. Schubert, A. Venugopal, M. J. Kahlich, V. Plzak, and R. J. Behm, J. Catal. **222**, 32 (2004).
[28] B. Schumacher, Y. Denkwitz, V. Plzak, M. Kinne, and R. J. Behm, J. Catal. **224**, 449 (2004).
[29] H. Huber, D. McIntosh, and G. A. Ozin, Inorg. Chem. **16**, 975 (1977).
[30] T. Venkov, K. Fajerwerg, L. Delannoy, H. Klimev, K. Hadjiivanov, and C. Louis, Appl. Catal., A **301**, 106 (2006).
[31] B. Hammer *et al.*, Phys. Rev. B **59**, 7413 (1999).